

FLAT BEAM GENERATION WITH THE PHASE SPACE ROTATION TECHNIQUE AT KEK-STF

M. Kuriki*, S. Aramoto, Z. Liptak, Hiroshima U. ADSE, Higashihiroshima, Japan
H. Hayano, X. Jin, Y. Seimiya, N. Yamamoto, Y. Yamamoto, KEK, Tsukuba, Japan
S. Kashiwagi, Tohoku U. ELPH, Sendai, Japan
K. Sakaue, U. of Tokyo, Tokyo, Japan
M. Washio, Waseda U., Tokyo, Japan

Abstract

Flat beam generation from angular momentum dominated beam with a phase-space rotation technique is an unique method to manipulate the phase-space distribution of beam. As an application, the asymmetric emittance beam generation for linear colliders is considered to compensate the Beamstrahlung effect at Interaction point. By using this technique, the asymmetric beam can be generated directly with the injector, instead of radiation damping with a damping ring. We present the result of a proof-of-principle experiment at KEK-STF.

INTRODUCTION

Electron Positron Collider is the only way to realize annihilation of elementary particles with controlled conditions with the current technology. Because there has been no any significant evidence of Super-symmetry in LHC experiments, the significance of detail studies of Higgs boson and searching inconsistency in the standard model with electron positron collider is maximized. ILC (International Linear Collider) [1] is an e+e- linear collider based on superconducting accelerator with center of mass energy from 250 to 1000 GeV. It would be constructed in Iwate, Japan, as the main project of High energy physics.

Luminosity L of linear colliders is

$$L = \frac{fn_b N^2}{4\pi\sigma_x\sigma_y}, \quad (1)$$

where f is repetition of pulse, n_b is number of bunches in a pulse, N is number of particles in a bunch, $\sigma_{x,y}$ is transverse beam size. In the linear collider, the beam after the collision is not recycled. If we employ a large current beam in linear colliders as same as in ring colliders, the required wall plug power is huge and such machine is unrealistic. One way to enhance the luminosity with a limited electricity is minimizing $\sigma_{x,y}$, but it causes a large energy spread by Beamstrahlung which is proportional to $(\sigma_x + \sigma_y)^{-2}$. A practical way to enhance the luminosity and suppress Beamstrahlung simultaneously is squeezing the beam in one of the transverse direction, e.g. $\sigma_x \gg \sigma_y$. For ILC, The beam size at interaction point, IP is 640 nm in horizontal direction and 5.7 nm in vertical direction. Emittances are 10 and 0.04 mm.mrad in horizontal and vertical directions, respectively [1]. This asymmetric emittance beam is made by

radiation damping in a storage ring (damping ring) in the current design. The ring has to accommodate all bunches in one pulse, 1300 bunches and the circumference is 3 km.

We propose to generate the flat beam for ILC only with the injector by employing the emittance exchange technique and omitting the 3km storage ring. There are two methods as the phase-space rotation for the re-partitioning. One is RFBT (Round to Flat Beam Transformation) [2] generating a flat beam from an angular-momentum dominated beam produced by beam emission in a solenoid field. Another is TLEX (Transverse to Longitudinal Emittance eXchange) exchanging the phase-spaces between longitudinal and transverse directions by dipole mode cavity in a dispersive beam line [3]. These two techniques are experimentally demonstrated by P. Piot et al. [4] for RFBT and Y-E Sun et al. [5] for TLEX. The flat beam generation with RFBT and TLEX are explained in Ref. [6] for more detail. We propose the flat beam generation with the emittance exchange techniques, RFBT and TLEX as shown in Fig. 1. In the first part, the

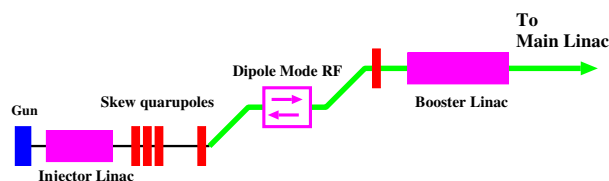


Figure 1: The injector design employing the emittance exchange techniques, RFBT and TLEX.

repartitioning between ϵ_x and ϵ_y by RFBT is performed. In the following section, TLEX exchanges ϵ_x and ϵ_z . The emittance budget is summarized in Table1. The first row is required emittance at IP for ILC. The second row is emittance at Gun when we employ only RFBT. In RFBT, the product of ϵ_x and ϵ_y is conserved. To make 10 mm.mrad and 0.04 mm.mrad only with RFBT, the emittance from Gun should be 0.6 mm.mrad in x and y directions. This small emittance cause several problems, e.g. emittance growth by space charge, a long bunch from gun due to the limited emission area, etc.

The third row shows the emittance at gun when we employ RFBT and TLEX as shown in Fig.1. If we employ RFBT and TLEX, the product of three emittance (x, y, and z) can be conserved and therefore, the initial ϵ_x and ϵ_y can be large to avoid the problem at the gun emission and the space charge emittance growth. The fourth row shows the

* mkuriki@hiroshima-u.ac.jp

Content from this work may be used under the terms of the CC BY 4.0 licence (© 2022). Any distribution of this work must maintain attribution to the author(s), title of the work, publisher, and DOI

Table 1: Emittance Budget for ILC at IP (TDR), Case 1 (Only RFBT, Gun), Case 2 (RFBT and TLEX, Gun), and Case 2 (RFBT and TLEX, IP) (Emittance is in mm.mrad)

Design	ϵ_x	ϵ_y	ϵ_z
ILC at IP (TDR)	10	0.04	2.5×10^5
Case 1 (RFBT, gun)	0.6	0.6	2.5×10^5
Case 2 (RFBT+TLEX, gun)	45	45	10
Case 2 (RFBT+TLEX, IP)	10	0.04	5.1×10^4

expected emittance with the same parameter at IP. ϵ_x and ϵ_y are compatible to the ILC requirement at IP. ϵ_z becomes large comparing to the initial value at gun, but it is still less than the requirement.

BEAM TEST AT KEK-STF

To demonstrate this method, we carried out a pilot experiment at KEK-STF (Super-conducting Test Facility). Figure 2 shows the STF beam line schematically. Electron beam is generated by 1.3 GHz L-band normal conducting RF gun [7], designed by DESY and fabricated by FNAL. The peak field is 44 MV/m with 3.5 MW RF input [8].

The cathode is Cs_2Te semiconductor formed on a molybdenum block by evaporation in vacuum. The laser spot size is 1.0 mm in radius. The wave length is 266 nm. The expected beam emittance is 0.85 mm.mrad.

Solenoid field has a crucial role in RFBT. In nominal case, solenoid field has to be zero on the cathode to prevent the emittance growth. In this study, the solenoid field has to be set to make the angular momentum. The gun solenoid magnet composed from a main coil and a bucking coil. In nominal operation, the main and bucking coils are operated different polarity, but we switched the polarity of the bucking coil to make a solenoid field on the cathode. The solenoid field can be up to 0.1 Tesla by the switching.

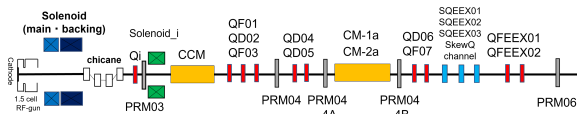


Figure 2: A schematic view of STF beam line.

Chicane orbit is placed at the downstream of RF gun for the laser right angle injection. CCM stands for capture cryomodule which accommodates two super-conducting cavities. The cavity is 1.3 GHz TESLA type 1.3 m 9 cell cavity which generates 30 MV/m accelerating field. Between CCM and CM-1a and CM-2a, a beam diagnostic section is placed. In this section, emittance can be measured by Q-scan method in the middle with PRM04 screen and in the end with PRM04-4A screen. Even it is not drawn, there is a momentum analyzer with a bending magnet in the middle.

CM-1a and CM-2a are cryomodule and they are connected as a long cryomodule. In CM-1a and CM-2a, there are 9 TESLA cavities with 40 MV/m gradient.

Table 2: STF Simulation Parameters for RFBT

Parameter	value	unit
RMS Beam size	1.1	mm
RMS laser pulse length	5.1	ps
RF gun peak E_z	46.5	MV/m
B on cathode	280	Gauss
CM1 cavity peak E_z	30	MV/m
CM2 cavity peak E_z	40	MV/m

At the downstream of CM-2a, the section is called as RFBT section composed from two Q-magnets, three skew Q magnets, two Q-magnets, and RPM06 (screen). The Q magnets adjust Twiss parameters at the first skew Q magnet symmetry in x and y. This is a requirement for RFBT. The three skew Q magnets play the primary roles of resolving correlations induced by the solenoid field on the cathode and generating asymmetric emittance [9]. The emittance after the skew Q magnets ϵ_{\pm} are

$$\epsilon_{\pm} = \sqrt{\epsilon_{th} + (\kappa \sigma^2)^2} \pm \kappa \sigma^2 \quad (2)$$

where ϵ_{th} is thermal emittance of cathode, κ is correlation by the solenoid field between x and y' and y and x' , σ is the beam size at the cathode. ϵ_+ and ϵ_- are the large and small emittance at the exit of the skew Q magnets. The product of the emittance is conserved as ϵ_{th}^2 and the ratio is

$$\frac{\epsilon_+}{\epsilon_-} = \left(\frac{\kappa \sigma^2}{\epsilon_{th}} \right)^2 \quad (3)$$

Table 2 summarizes the parameters for RFBT at STF.

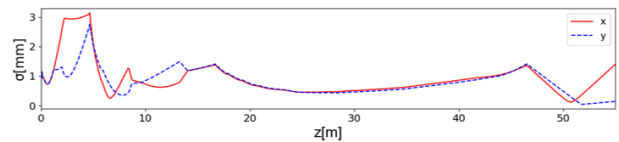


Figure 3: Beam size evolution along STF beam line evaluated with the simulation. The solid and dotted lines show σ_x and σ_y , respectively.

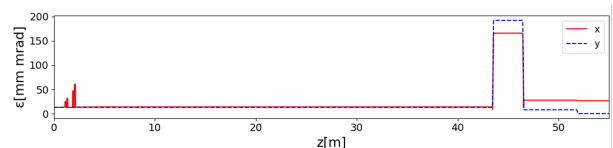


Figure 4: Emittance evolution along the STF beam line evaluated with the simulation. The solid and dotted lines show ϵ_x and ϵ_y , respectively.

Figures 3 and 4 show the beam size and emittance obtained by simulation. The solid and dotted lines show σ_x and σ_y or ϵ_x and ϵ_y . ϵ_y becomes small at the exit of the skew Q magnets as a result of RFBT.

Table 3: Expected Emittance RFBT at STF

Parameter	Simulation	Theory	Unit
ϵ_x	26.6	26.2	mm.mrad
ϵ_y	0.13	0.030	mm.mrad
ϵ_x/ϵ_y	200	870	

Table 3 summarizes the results of the simulation. Theory value is the expected value according to Eq. (3). Due to the emittance growth effect by space charge, the emittance ratio by simulation is 200 which should be compared with 870 by the theory according to Eq. (3).

RFBT experiment was carried out at KEK-STF on Dec. 2021. The procedures of the RFBT experiment are

1. Beam operation with zero B_z field on cathode (solenoid field).
2. Set the symmetric beam optics and confirm Twiss parameter at the down stream. The symmetric beam optics means Twiss parameter is symmetric in x and y. To confirm the Twiss parameters, skew Q magnets (SQEEX01, SQEEX02, and SQEEX03 in Fig. 2) are turned off. Twiss parameters are measured by Q-scan with QFEEX01 and QFEEX02.
3. Set non-zero B_z at the cathode for RFBT experiment.
4. Set skew Q magnets according to the simulation.
5. Optimize the skew Q magnets to obtain the minimum ϵ_y .

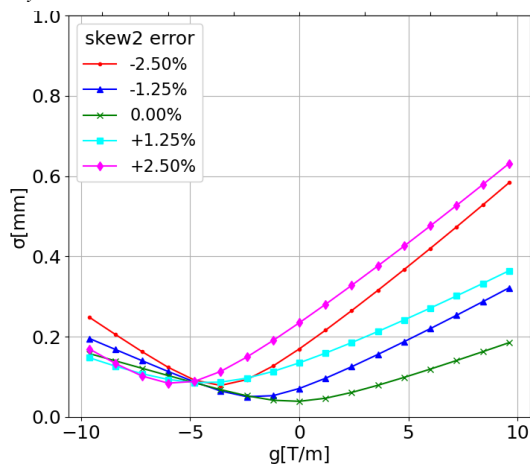


Figure 5: Q-scan curve at the RFBT section with errors on skew Q magnets. Skew 1 and skew Q are set with +2.5% and -10% currents, respectively. Those curves are drawn with skew Q 2 errors from -2.5% to +2.5 %.

Figure 5 shows an example of Q-scan plot for the skew-Q tuning. The curve is drawn with skew-Q magnets with errors; Skew Q 1 and skew Q 3 are set + 2.5% and -10% with respect to the optimum value. Those curves are drawn with different errors on Skew Q 2, from -2.5% to +2.5%. According to the plots, 0 % error, i.e. optimum setting gives the lowest waist size in the Q-scan. By repeating such measurements, the skew Q magnet currents can be optimized.

Table 4: Emittance and Twiss Parameter Measurement at QF03 and QD05

Parameter	QF03	QD05	Unit
ϵ_x	4.0 ± 0.1	14.5 ± 0.6	mm.mrad
ϵ_y	6.0 ± 0.3	27.8 ± 16.8	mm.mrad
α_x	0.52 ± 0.1	7.8 ± 0.3	
α_y	10.6 ± 0.5	1.3 ± 1.4	
β_x	2.6 ± 0.1	1.3 ± 0.1	m
β_y	6.6 ± 0.33	0.2 ± 0.1	m

Figure 6 show Q-scan results with QF03 and QD05 in horizontal direction. The emittance measurement at those magnets are summarized in Table 4. As shown in Fig. 2, QF03 ad QD05 are in the middle of STF beam line, between CM1 and CM2. According to the measurements, a significant emittance growth was occurred between QF03 and QD05.

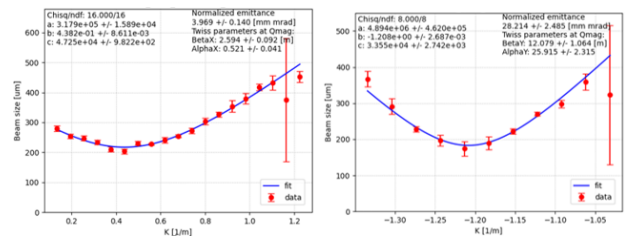


Figure 6: Q-scan plot measured with QF03 (left) and QD05 (right) in horizontal direction (x) giving $\epsilon_x = 3.97 \pm 0.14$ mm.mrad and $\epsilon_x = 14.5 \pm 0.6$ mm.mrad respectively.

Due to the emittance growth in the middle of STF beam line, RFBT experiment at KEK-STF was not completed. Currently, we investigate the reason of the emittance growth. After solving this problem, the experiment will be carried out again in this year.

SUMMARY

A new method to generate a high aspect ratio beam for linear colliders employing the 6D phase-space rotation is discussed. Starting from a large beam size in transverse direction, ILC required beam can be generated by emittance repartitioning in 6D phase space by RFBT and TLEX avoiding emittance growth due to space charge effect. As a demonstration of the asymmetric beam generation with RFBT, an experiment at KEK-STF was carried out. In the experiment, a significant emittance growth was observed and the position was identified at the middle of the beam line, between QF03 and QD05, but the reason is not understood yet. After solving this problem, the experiment will be carried out again.

ACKNOWLEDGEMENTS

This work is partly supported by Grant-in-Aid for Scientific Research (B).

REFERENCES

- [1] “ILC Technical Design Report”, KEK-Report 2013-1, 2013.
- [2] R. Brinkmann *et al.*, “A low emittance, flat-beam electron source for linear colliders”, *Phys. Rev. ST Accel. Beams*, vol. 4, p. 053501, 2001. doi:10.1103/PhysRevSTAB.4.053501
- [3] M. Cornacchia and P. Emma, “Transverse to longitudinal emittance exchange”, *Phys. Rev. ST Accel. Beams*, vol. 5, p. 084001, 2002. doi:10.1103/PhysRevSTAB.5.084001
- [4] P. Piot, Y.-E Sun, and K.-J. Kim, “Photoinjector generation of a flat electron beam with transverse emittance ratio of 100”, *Phys. Rev. ST Accel. Beams*, vol. 9, p. 031001, 2006. doi:10.1103/PhysRevSTAB.9.031001
- [5] Y.-E Sun *et al.*, “Tunable Subpicosecond Electron-Bunch-Train Generation Using a Transverse-To-Longitudinal Phase-Space Exchange Technique”, *Phys. Rev. Lett.*, vol. 105, p. 234801, 2010. doi:10.1103/PhysRevLett.105.234801
- [6] M. Kuriki *et al.*, “High Luminosity Flat Beam Generation With Phase-space Rotation for Linear Colliders”, in *Proc. of PASJ*, Nagaoka, Japan, Aug. 2018, paper THOM07.
- [7] H Sugiyama *et al.*, “L-band Photocathode RF Gun at KEK-STF”, in *J. Phys.: Conf. Ser.*, vol. 298, p. 012015, 2011. doi:10.1088/1742-6596/298/1/012015
- [8] M. Kuriki, “1 ms pulse beam generation and acceleration by photocathode Radio Frequency Gun and Superconducting accelerator”, *Jpn. J. Appl. Phys.*, vol. 52, p. 056401, 2013. doi:10.7567/JJAP.52.056401
- [9] M. Kuriki *et al.*, “Effect of Initial Parameters on the Super Flat Beam Generation with the Phase-Space Rotation for Linear Colliders”, in *Proc. IPAC'19*, Melbourne, Australia, May 2019, pp. 442–444. doi:10.18429/JACoW-IPAC2019-MOPMP009